Macromolecules
ARTICLE

Macromolecules **2010**, *43*, 9087–9093 **9087**
DOI: 10.1021/ma1013429

Effect of Molecular Weight and Arm Number on the Growth and pH-Dependent Morphology of Star Poly[2-(dimethylamino)ethyl methacrylate]/Poly(styrenesulfonate) Multilayer Films

Zhizhang Guo, Xingyu Chen, Jianyu Xin, Duo Wu, Jianshu Li,* and Chenlong Xu

College of Polymer Science and Engineering, Sichuan University, Chengdu 610065, China

Received June 17, 2010; Revised Manuscript Received September 25, 2010

ABSTRACT: The influence of molecular weight and arm number of star polymers on the buildup and pH-dependent morphology changes of multilayer films assembled from star poly[2-(dimethylamino) ethyl methacrylate] (PDMAEMA) and linear poly(styrenesulfonate) (PSS) was systematically investigated. Well-defined star PDMAEMA, consisting of β-cyclodextrin (CD) core and different arm number (21, 14, and 7) were successfully synthesized via atom transfer radical polymerization (ATRP). It is found that star polymers with certain arm number deposit more mass with the increase of molecular weight. As for the star polymers with almost the same arm length but different arm number, film assembled from 14-arm star PDMAEMA exhibits the fastest growth and the most significant morphology changes upon the pH 2.75 treatment. It is assumed that the interdiffusion of PSS controlled by star PDMAEMA with different structures should be responsible for the different buildup and pH-dependent morphology changes of the multilayer films.

Introduction

The layer-by-layer (LbL) deposition technique initially introduced by Decher et al. in the early 1990s has been the prime choice for constructing nanoscale films on a surface.[1−3] As a versatile and tunable method, it has rapidly attracted the most attention over a wide range of materials science. Besides conventional polyelectrolytes, inorganic nanoparticles,[4] dendrimers,[5] carbon nanotubes,[6] and biological substances such as DNA,[7] proteins,[8] and viruses[9] have been successfully used as building blocks for LbL multilayer films. The increasing kinds of LbL component materials based on various driving forces further enriched their potential application in several areas, including controlled drug release,[10] solar cells,[11] biomaterial coatings,[12] catalysts,[13] and biosensors.[14] In recent years, much effort has been made to gain further understanding of the factors that govern the multilayer buildup process.[15,16] Hyperbranched polymers, especially dendrimers[5,17] and star polymers,[18−20] have been introduced into multilayer thin films due to their unique conformation and nanostructural functionality. Some precursory researches demonstrated that LbL deposited films constructed by dendrimers or star polymers behaved quite differently from those of their linear counterparts with equivalent compositions. It was concluded that the star structure of the polyelectrolytes play a crucial role in controlling the formation and the resulting properties of LbL multilayer films.[19,20]

Star polymers are characterized as a globular shape with a number of arms radiating from a central core. The starlike polymers can basically be synthesized using two different strategies: "arm-first" and "core-first". The "arm-first" approach consists of reacting preformed living linear polymers (arms) with a multifunctional quencher molecule that forms the core of the star. Star polymers can also be prepared via the "arm-first" method if the arms and multifunctional coupling reagent contain complementary functionalities. In contrast, the alternative "core-first" method involves using a multifunctional initiator to initiate polymerization, which has been applied successfully to acquire well-defined star polymers with precise arm numbers. Meanwhile, controlled/living radical polymerization,[21] including atom transfer radical polymerization (ATRP), has been demonstrated to be an efficient technique for synthesizing star polymers with well-defined structure,[22−24] arm chain length in particular. Further, star polymers could be easily modified to have temperature-, pH-, or other stimuli-responsive functionalities, which would be applied to modulate the assembly and mechanical properties of LbL multilayer films by varying the nanoenvironment conditions. Connal et al.[19] have utilized poly(allylamine hydrochloride) (PAH) and pH-responsive poly(acrylic acid) (PAA) core cross-linked star polymers to prepare LbL films. The star PAA/PAH films showed distinct morphology changes in response to post-treatment with different pH solutions. The assembly behavior of pH-responsive all-star polymer multilayer films was also investigated and compared to linear polyelectrolytes by Kim et al.[20]

The above studies have fully demonstrated the promising applications of star polymers in multilayer films. However, the effects of molecular weight (MW) and arm number of star polymers on the formation of LbL films have not been discussed yet. In this work, a series of well-defined star poly[2-(dimethylamino)ethyl methacrylate] (PDMAEMA) with different molecular weight and arm number were synthesized via ATRP through "core-first" method. The ATRP initiators with designed initiation sites (21, 14, and 7) were prepared according to our previous work.[25] The multilayer thin films are prepared by the alternate LbL deposition based on electrostatic interactions between positively charged star PDMAEMA and negatively charged linear poly(styrenesulfonate) (PSS). We report, to the best of our knowledge, the first example of investigating the effects of star polymer architecture on the assembly, morphology, and pH-responsivity of LbL membrane. The growth approaches and pH-dependent morphology changes of these films are demonstrated and compared, which will be helpful for further understanding the internal arrangement of the star-polymer-based LbL films during their buildup and post-treatments.

*Corresponding author. E-mail: jianshu_li@scu.edu.cn.

Published on Web 10/14/2010

Scheme 1. Synthesis of Star PDMAEMA via ATRP from Per-2,3-di-*O*-chloroacetyl-β-cyclodextrin (14Cl-β-CD)

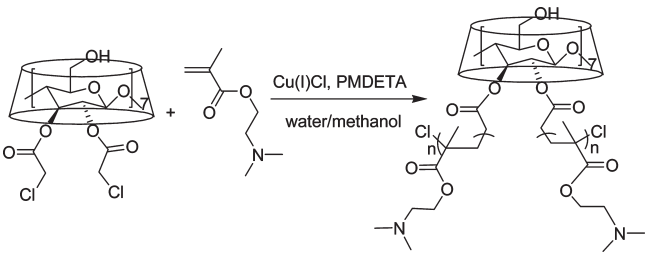

Experimental Section

Materials. Poly(styrenesulfonic acid) sodium salt (PSS, M_w 70 000 g/mol) was purchased from Alfa Aesar. 2-(Dimethylamino) ethyl methacrylate (DMAEMA, 99%, Aladdin Reagent Co., Ltd., China) was purified by passage through a column of activated basic alumina to remove inhibitor. Chloroacetylated β-cyclodextrins (21-, 14-, and 7Cl-β-CD, Supporting Information) were prepared as multifunctional ATRP initiators according to our previous work.[25] *N,N,N′,N″,N″*-Pentamethyldiethylenetriamine (PMDETA; 98%) was purchased from J&K Chemical Ltd. (Beijing, China). Copper-(I) chloride (CuCl; 97%) was stirred in glacial acetic acid, filtered, then washed promptly with absolute ethanol, and dried under vacuum. All other reagents were of analytical grade or higher and used as received unless stated otherwise. Quartz crystal microbalance (QCM) electrodes (titanium/gold crystals, resonant frequency = 5 MHz) were of Stanford Research System Corp. products. A home-built QCM, constructed using a model QCM 100 analogue controller (Stanford Research System products Corp.) and an Agilent 53131A universal counter, was employed for the microgravimetric experiments. The quartz wafers (10×30 mm^2) were cleaned following the "RCA clean" protocol to hydrophilize the surfaces using the method described by Connal et al.[19] Ultrapure water produced from a Milli-pore system with a resistivity higher than 18.2 M$\Omega\cdot$cm was used in all the experiments.

Syntheses of Star PDMAEMA Polymers via ATRP. A representative process for the polymerization of DMAEMA using the 14Cl-β-CD initiator was described as follows (Scheme 1). The reaction was performed in a 50 mL three-necked flask with magnetic stirring. Distilled DMAEMA (3.6 mL, 21.4 mmol), 14Cl-β-CD (22 mg, 0.01 mmol), and PMDETA (100 μL, 0.42 mmol) were dissolved in 2.7 mL of a methanol/water (7/1, v/v) mixture. After three freeze−pump−thaw cycles, the reaction mixture was further degassed by bubbling nitrogen for 20 min. Then, CuCl (42 mg, 0.42 mmol) was added into the flask under a nitrogen atmosphere. As the CuCl dissolved gradually, the solution turned to brilliant blue. The reaction was then kept at 25 °C for 8 h. Sample was taken from the rubber stopper for ^{1}H NMR analysis. The polymerization was terminated by exposing to air and diluted with 50 mL of THF. A colorless solution was obtained after catalyst complex was removed by passing through a short basic alumina column. After being concentrated in a rotary evaporator, the solution was poured into excess cold *n*-hexane for precipitation, yielding white solid. Then, star polymers were collected and dried under vacuum at 40 °C for 2 days.

Characterizations of Star PDMAEMA. Gel permeation chromatography (GPC) measurement was performed on a Waters GPC system equipped with Ultrahydrogel columns and Waters 410 differential refractometer detector at 25 °C. Water was used as the eluent, and the flow rate was 1.0 mL/min. Calibration was made using standard monodispersed poly(ethylene glycol) (PEG). Dynamic light scattering (DLS) analysis was carried out on a Brookhaven BI-200 SM system incorporating a He−Ne laser (λ = 532 nm) at 25 °C. The hydrodynamic diameters of polymer at a concentration of 10 mg/mL in water (pH varying from 10 to 2) were collected three times at an angle of 90°. The apparent charge density of star PDMAEMA was determined using a Mütek particle charge detector (Herrsching, Germany). After filtrated with 0.45 μm microporous filter, 0.2 mL of star polymer solution (0.5 mg/mL, pH = 6.0) was added into the sample cell and diluted with water to 10 mL. The titration was carried out with a standard anionic polyelectrolyte (potassium poly(vinyl sulfate) (PVSK)) solution (concentration = 1 mM). Three repeats were performed to get the average value for each sample.

Assembly of Star PDMAEMA/PSS Multilayer Films. The aqueous solutions of star PDMAEMA (0.5 mg/mL, 0.1 M NaCl, pH = 6.0) and PSS (0.5 mg/mL, 0.1 M NaCl, pH = 6.0) were prepared and filtrated with 0.45 μm Nylon Cameo filtersyringe prior to use. The substrate of cleaned quartz was initially immersed into the PDMAEMA solution for 10 min and rinsed by consecutively three dips in Milli-Q water for 1 min each, followed by drying with nitrogen airgun before performing data collection. Then the substrate was dipped into PSS solution for 10 min and followed with the same rinsing and drying steps as described above. Film with certain number of layers was obtained by alternating sequential adsorption in PDMAEMA and PSS solutions. A bilayer is defined as a layer of polycation and polyanion, and the half-integer number of bilayer means that the film ends with star PDMAEMA as the outermost layer. The films prepared for QCM analysis were manufactured by dropping and extending 200 μL solution onto a certain area of the QCM electrode using a pipet instead of immersing it into the polyelectrolyte solution. All experiments were carried out at room temperature in an air-conditioned room.

Characterizations of LbL Multilayer Film. UV/vis spectra was performed with a Mapada UV-1800PC spectrophotometer. The absorbance of PSS at 262 nm was recorded after each adsorption step. Assembly steps were also monitored by a home-built QCM device with a frequency counter. An Inspect F scanning electron microscopy (SEM) was used to observe the surface and cross-section morphology, operating at 10.0 keV. For the atomic force microscopy (AFM) measurements, a SPA400 Digital Instrument equipped with SI-DF20 Micro cautilever was used. All AFM images of multilayer films were captured in tapping mode (TM-AFM) with spring constant of 12 N/m and resonant frequency of 127 kHz. The root-mean-square (rms) of the surface roughness data were collected from three imaging area of 5×5 μm^2.

Results and Discussion

The controlled polymerization of DMAEMA monomer via ATRP in nonpolar solvents was first reported by Zhang et al.[26] After then, Mao and co-workers[27] have discussed the efficient polymerizations of DMAEMA via ATRP in various methanol and water mixtures at room temperature. The synthesis of PDMAEMA with molar mass up to 1 million was also successfully achieved by Mao et al.[28] The solvent mixture of methanol and water was fixed at 7/1 (volume ratio) in this work. The well-defined star polymers, consisting of β-cyclodextrin (CD) core and different number of PDMAEMA arms, were successfully synthesized via ATRP using the "core-first" method. For example, the monomer conversion and yields while preparing S5 was 65% and 45%, respectively, as shown in Figure 2 of the Supporting Information. The reaction conditions and GPC results of PDMAEMA star polymers are summarized in Table 1. The polydispersity index (PDI) value of star polymers remains low, indicating the well-controlled polymerization (Supporting Information).

As shown in Table 1, star polymer S1−S4 have 21 arms but different arm chain length. Meanwhile, samples S2, S5, and S6 are designed to have the same number of DMAEMA repeat units per arm, which are 93, 87, and 88 calculated from M_n, respectively. These star polymers have very similar arm length but different arm number. The arms are connected to the CD core via ester linkages, which could be cleaved by hydrolyzation under basic conditions. To determine the number of star polymer arms, star polymer S1 was chosen and hydrolyzed with a potassium hydroxide solution in a mixture of THF and methanol at 40 °C for 2 days, at which

Table 1. Polymerization Conditions, GPC, and Charge Density Results of Star PDMAEMA Samples

PDMAEMA samples	arm number[a] (n_{arm})	$[M]_0/[I]_0/[Cu]_0/[L]_0$[b]	time (h)	M_n	M_w/M_n	charge density ($\times 10^{-5}$ equiv/g)
S1	21	230/1/3/3	8	393 500	1.19	74.1 ± 0.6
S2	21	160/1/3/3	8	310 900	1.13	85.8 ± 1.7
S3	21	110/1/3/3	8	227 400	1.10	86.9 ± 1.1
S4	21	55/1/3/3	8	95 100	1.17	92.1 ± 2.1
S5	14	160/1/3/3	8	194 000	1.09	39.7 ± 2.4
S6	7	160/1/3/3	8	98 800	1.12	43.4 ± 1.5

[a] Determined by ATRP initiators with designed initiation sites (21-, 14-, and 7Cl-β-CD). [b] $[M]_0$, $[I]_0$, $[Cu]_0$, and $[L]_0$ represent the initial malor ratio of monomer, total initiation sites of different initiators, Cu(I)Cl, and ligand (PMDETA), respectively.

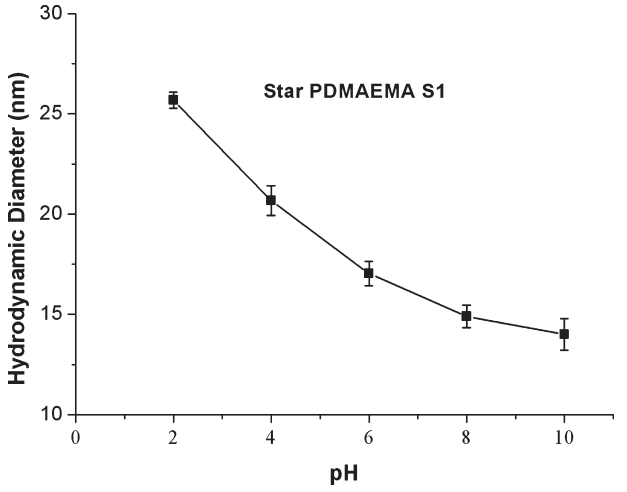

Figure 1. Hydrodynamic diameters (D_H) of star PDMAEMA at different pH conditions. The concentration of star polymers S1 was 10.0 mg/mL.

condition hydrolysis is restricted to the esters joining the arms to the core and does not affect the main polymer chains (see Figure 4 of the Supporting Information). After hydrolysis, the M_n and PDI of the polymer arms measured by GPC were 17 400 and 1.47, respectively. Taking into account of the M_n of the original star polymer S1 and CD core initiator molar mass (M_n 1135), the number of arms is estimated to be 22.5, which is rather close to the designed 21 arms. Meanwhile, the absolute M_w of star polymer S1 and linear arm polymer obtained by multiangle laser light scattering (MALLS) detector (Supporting Information) were 490 100 and 20 600 g/mol, respectively. Thus, the number of arms is estimated to be 23.7. The disparity of M_w obtained from MALLS and GPC measurement may due to the dense structure of star polymer compared to the linear polymer of similar molecular weight.

The effective pK_a of the DMAEMA star polymers shows slightly disparity from their linear counterparts. For example, the pK_a of star S1 shifts from 7.5 (linear[29]) to 6.5 (measured by potentiometric titration, data not shown). This is because of the higher inner osmotic pressure caused by the more compact charged groups due to the unique architecture of star polymers.[20] That is, to reach the same degree of ionization, more protons are needed to overcome the higher pressure and penetrate the congested structure to access the inner of star polymers. The pH-responsive behavior of star PDMAEMA is demonstrated by dynamic light scattering as shown in Figure 1. The average hydrodynamic diameters (D_H) of star polymer change along with the varying of pH. With the decrease of pH from 10 to 2, the D_H of star PDMAEMA S1 increases from 14 to 26 nm. The star polymers are in a constrained coiled conformation at high pH. While the protonation degree of DMAEMA arms increases, the star

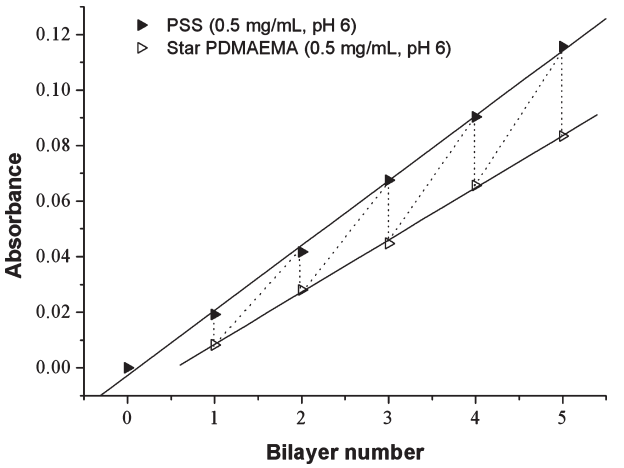

Figure 2. Absorbance of PSS at 262 nm versus the number of star PDMAEMA/PSS bilayers. The absorbance of the first layer (star S1) deposited on quartz substrate corresponds to zero. All of the polymer solutions were made with 0.1 M NaCl. The dotted line indicates the stepwise PSS adsorption/extraction process.

polymer become more stretched due to the electrostatic repulsion between the chains.

The exponential growth mode of polyelectrolyte multilayers has been studied by several groups,[30,31] and then the so-called "in and out" diffusion buildup mechanism has been widely accepted. The thickness of star PDMAEMA and linear PSS LbL films investigated by QCM measurement also increases exponentially with the bilayer number, which would be related to the diffusion ability of at least one of the polyelectrolytes. Because of its globular structure and higher molecular weight, star polymer is unlikely to be the diffusion species in the multilayer film.[18]

The layer-by-layer sequential depositions of the two polyelectrolytes are demonstrated both by UV/vis adsorption spectroscopy and QCM. It has been reported by Kim et al. that PDMAEMA could be well-covered on silicon wafer.[20] Therefore, star polymers, not the branched PEI, were deposited on the quartz surface as the first layer in this work. The adsorption and desorption behavior of dye molecules in alternating deposited LbL films has been reported by Tedeschi et al.[32] The highly identical trend was also found in our experiments as presented in Figure 2. The maximum absorption of PSS at 262 nm was chosen in order to avoid the interferer adsorption of PDMAEMA between 200 and 240 nm. The absorbance decreased after each star PDMAEMA layer was deposited. Meanwhile, the star PDMAEMA aqueous solution turned to be whitish after manufacturing several layers. It would be the electrostatic complexes formed between the star polymer in solution and the PSS extracted from the LbL films.

In the QCM experiment, the crystal resonance frequency changes are recorded to reflect the mass of adsorbed polyelectrolyte on the crystal surface. As depicted in Figure 3, the linear PDMAEMA/PSS exhibited a regular linear growth trend at 2 mg/mL with 0.1 M NaCl. However, a wavelike growth region was observed for star polymer at the same conditions after two bilayers. It seems that star polymers at higher concentration (2 mg/mL) could not be stably deposited onto the quartz crystal microbalance. The frequency increased after each deposition of star PDMAEMA, which indicates that the deposited mass was unexpectantly lost in the bilayer manufacturing cycle. No wavelike growth was found while the concentration was changed to 0.5 mg/mL (Figure 4). Thus, it is important to note that the polymer solutions should be prepared in certain concentration ranges for LbL assembly. A higher polymer concentration would not necessarily result in greater deposited mass. Also, the LbL thin films exhibit pH tunable growth due to the protonation

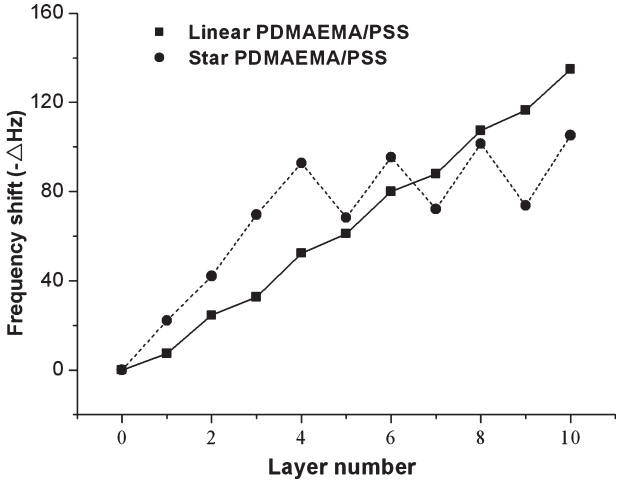

Figure 3. Frequency shifts on QCM electrodes as a function of the number of layers for star PDMAEMA and linear PDMAEMA (hydrolysis from star polymer) multilayer films. All of the polymer solutions were prepared at 2 mg/mL at pH 6 with 0.1 M NaCl.

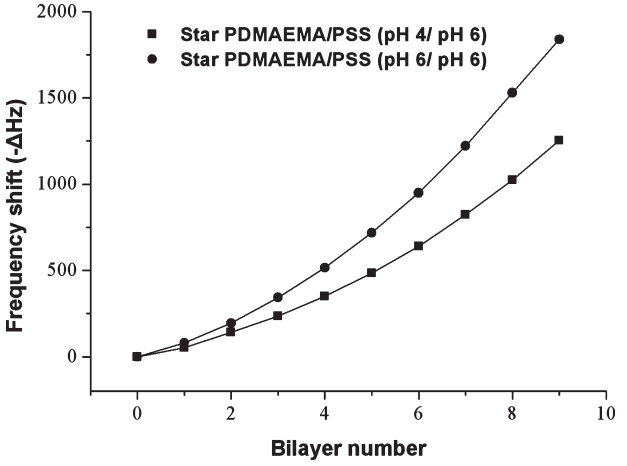

Figure 4. Exponential growth of S1/PSS at 0.5 mg/mL against the bilayer number of LbL films fabricating under different pH.

process of DMAEMA units on the star polymer chains. The pH of PSS solution was fixed at 6.0, while the S1 solutions were prepared at pH 4.0 and 6.0, respectively. As shown in Figure 4, the film fabricated under pH 6 was thicker than that prepared under pH 4. The following experiential equation is often used to estimate the film thickness from the frequency shift (ΔF).[33]

$$d\ (\mathrm{nm}) \approx -0.017\Delta F\ (\mathrm{Hz})$$

Thus, the film thicknesses of nine bilayers calculated from the total QCM frequency changes are 31.2 nm (pH = 6) and 21.3 nm (pH = 4). On the other hand, the pH-dependent growth agrees well with the conclusion drawn in previous work,[20,34] which have demonstrated that increasing the degree of ionization of a weak polyelectrolyte by controlling the dipping pH condition could result in thinner absorbed layers over a pH range.

The influence of the polyelectrolyte molecular weight on the exponential growth and morphology of multilayers has already been investigated with natural polysaccharides,[31] the hyaluronic acid/poly(L-lysine) (HA/PLL) and poly(L-glutamic acid)/poly(allylamine) (PGA/PAH) systems.[35] Recent advances of controlled/living polymerization techniques make it feasible to synthesize polymers with narrow polydispersity (PDI < 1.2), which is of great benefit to systematically investigate the influence of the

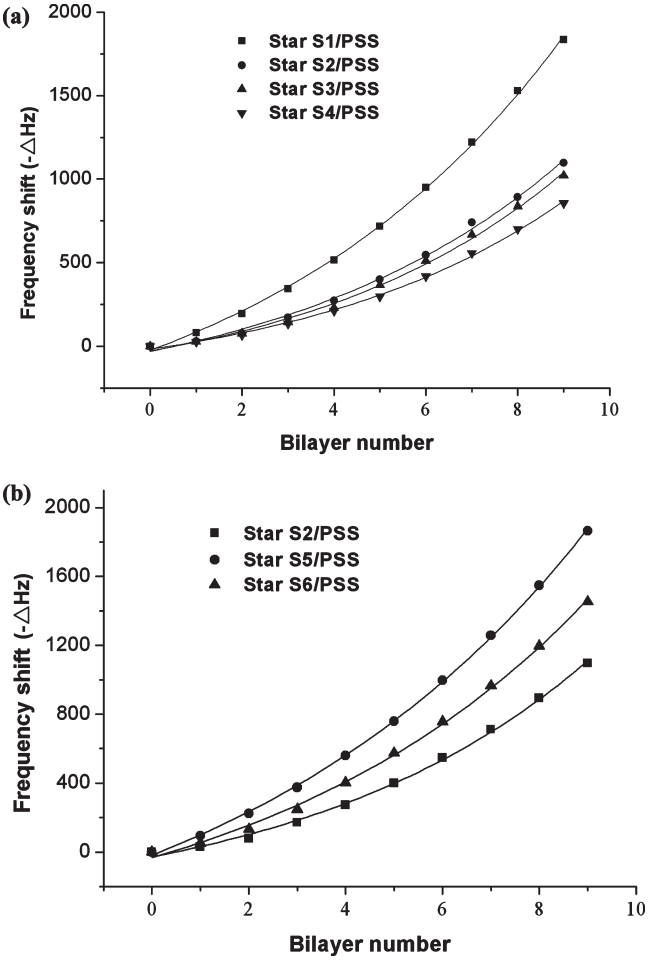

Figure 5. (a) QCM frequency shift versus the number of 21-arm star PDMAEMA/PSS bilayers prepared at pH 6/6. (b) QCM frequency shift versus the number of different arm star PDMAEMA/PSS bilayers prepared at pH 6/6.

molecular weight on several properties of multilayer films. It is found that 21-arm star polymer with longer chain length got more deposited mass for the same bilayers, calculating from the QCM frequency changes for films fabricated by S1−S4 (Figure 5a). Such difference in film growth is considered to be related to the diffusion movements within the films.[36] By using dye-conjugated polyelectrolytes, Picart et al.[30] have proved that the thickness of the new forming layer on top of the film is proportional to the amount of the free diffusion specie during the buildup process. In this work, it seems that the diffusion of PSS could significantly affect the thickness of multilayer films. In order to fully illustrate it, the charge density of each star polymer was measured as shown in Table 1. The higher apparent charge density would restrict the diffusion of PSS and decrease the amount of free PSS at the outer layer due to the higher degree of ionic cross-linking. Meanwhile, the lower extent of chain interpenetration between S1 due to its higher molecular weight and more congested architecture would be benefit to the diffusion of PSS and result in thicker films.

In this work, the investigation is focused on the influence of arm number of the star polyelectrolytes. The star PDMAEMA (S2, S5, and S6) with almost the same arm length but different arm number (21, 14, and 7, respectively) are chosen to carry out the QCM dissipation monitoring, together with AFM measurement. The frequency changes of each bilayer (pH 6/6) were recorded and are plotted in Figure 5b. As shown in Figure 5, the LbL film thickness calculated from QCM frequency changes (pH = 6) for S1−S6 was 31.2, 18.6, 17.4, 14.6, 31.7, and 24.7 nm, respectively. LbL

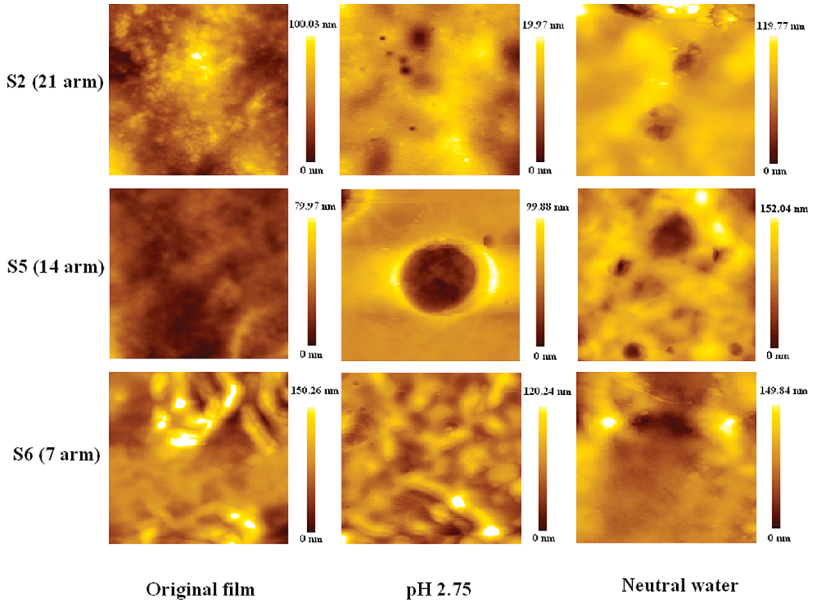

Figure 6. AFM images of different star PDMAEMA/PSS multilayer films before and after post-treatments. All the images areas are 5 × 5 μm^2.

assemblies of all the films follow the exponential growth pattern. Fourteen-arm star polymer (S5) shows the most amount of deposited mass for a given number of bilayers. Meanwhile, 21-arm star PDMAEMA (S2) gets the least deposited mass. It is obvious that the growth speed of star PDMAEMA/PSS multilayer films does not only depend on the molecular weight but also on other factors. Star PDMAEMA polymers with various arm number would achieve different protonation degree at certain pH/concentration due to their architectural difference. It is found that the sequence of apparent charge density under assembly condition is S2 > S6 > S5 (Table 1), which is reasonable to explain the deposited mass sequence of S2 < S6 < S5 (Figure 5) as the diffusion of negatively charged PSS is restricted by positively charged star polymer. However, the charge density might not be the only effect factor while we compare S1 with S5 as they exhibit close deposited mass although S1 has much higher charge density than S5. The higher molecular weight and more congested architecture of S1 could be another reason, which cause less polymer chain interpenetration and make the diffusion of PSS to be easier. Thus, both molecular weight and arm number of star polymers, which will result in different charge density and chain interpenetration at the pH/concentration condition of LbL assembly, may affect the buildup process and properties of LbL films.

The surface morphologies of multilayer films assembled from different star polymers are observed by AFM measurement (Figure 6). Also, the rms roughness data are presented in Figure 7. The films assembled from 21- and 7-arm star polymers have almost the same rms roughness (18.78 and 19.04, respectively). As the fastest growth system (see Figure 5), the film assembled from 14-arm star polymer (S5) exhibits the smoothest surface morphology. It seems that star polymer with lower charge density may result in the deposition of thicker and smoother film. The discrepancy may be caused by the different degree of protonation and the conformation of star polymers under the assembly conditions.

In general, the pH-driven thickness change and formation of large-scale porous morphology within the membrane are explained to be caused by structural rearrangement and phase separation of weak polyelectrolytes.[34,37,38] For star polymer, it has been reported that LbL multilayer film assembled with all star polymer exhibited more extensive pH-responsiveness upon the same post-treatment conditions compared with that assembled with their linear counterpart.[20] A reasonable explanation is that

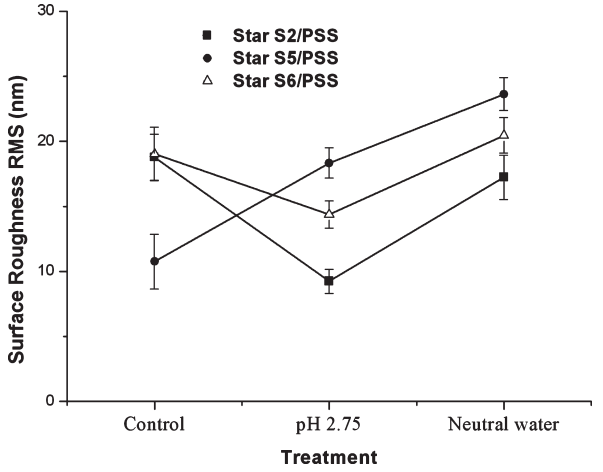

Figure 7. Surface roughness information on the films before and after post-treatments. The rms values are obtained from three different AFM images of 5 × 5 μm^2.

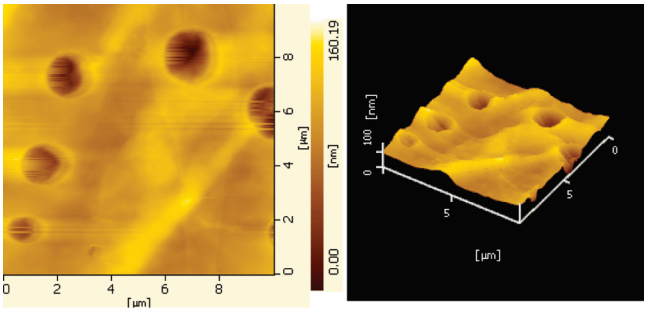

Figure 8. Large-scale AFM images of multilayer film assembled with 14-arm star polymer after being post-treated in pH 2.75 acidic solution for 30 min.

the star polyelectrolyte's compact structure can reduce the extent of interpenetration and the degree of ionic cross-linking between the multilayer assembly components.[20] The AFM measurement was performed to further investigate the pH-induced phase separation of multilayer films assembled from star polymer with different arm number. Each film undergoes remarkable thickness

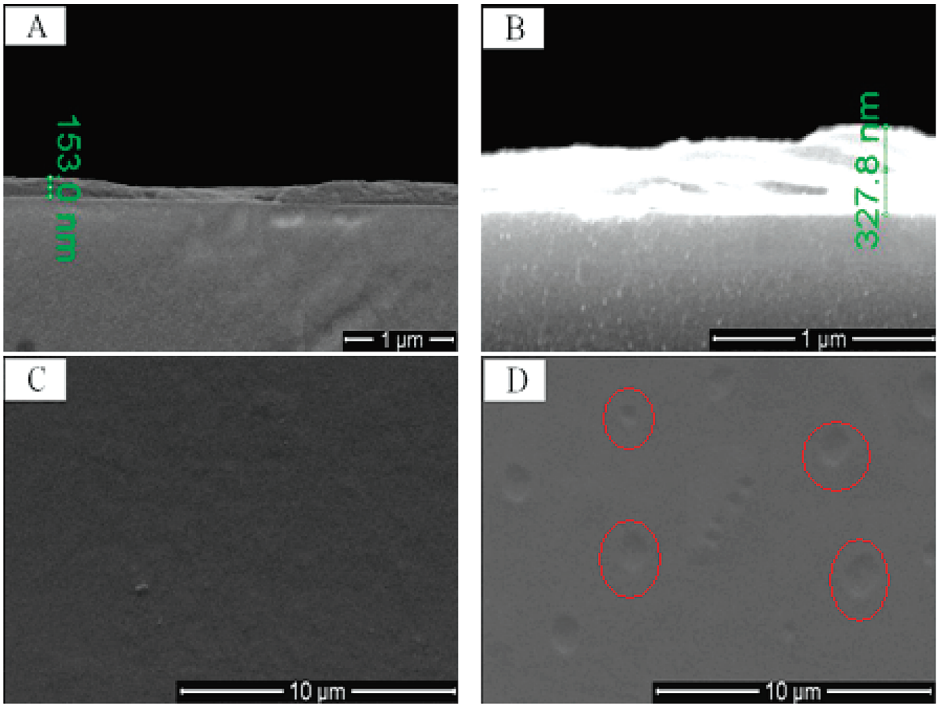

Figure 9. Morphology changes of star PDMAEMA/PSS film before (A, C) and after (B, D) post-treatment at pH 2.75. SEM cross section (A, B) and top-down (C, D) images are presented. The representative pores are labeled by red circles in (D).

swelling and surface morphology changes after being immersed into pH 2.75 acidic solution for 30 min and dried up at 120 °C for 2 h. At lower pH, the tertiary amine groups on the star PDMAEMA chains would become protonated gradually, which will disrupt a part of the original ionic cross-links and induce the as described spinodal-type decomposition.[40] The surface roughness of films assembled from 21- and 7-arm star polymers dereased after acidic treatment (Figure 7). The films were subsequently exposure to neutral water bath overnight to investigate the possible secondary reorganization. It is confirmed that the surface become rougher upon the neutral water treatment. These phenomena are consistent with the finding of previous work that smoother films are accompanied by the more stretched conformation of star polymers or vice versa.[19] As shown in column 2 of Figure 6, ununiform pores are observed within multilayer thin films deposited from 21-arm and 14-arm star polymers. It seems that star polymers with more arms can induce more notable morphology change upon the post-treatment due to the enlarged effect of the conformation transition from a swollen coil to a globule. In the AFM images, the smaller pores may indicate the initial stage of porosity transformation and pore development. It is interesting to find that the film fabricated with 14-arm star PDMAEMA exhibits the most significant morphology change with pore diameter up to 2 μm, and the surface turns to rougher upon the post-acidic treatment. Large-scale AFM images of $10 \times 10\ \mu m^2$ were captured, and several round pores of about 80 nm height were observed (Figure 8). It is hypothesized that star polymers with the lower charge density have less ionic binding sites when assembled into LbL films. Thus, the fracture of ionic cross-links and the structural rearrangement upon the post-acidic treatment may lead to more dramatic morphology change for 14-arm star polymer within the multilayer film.

The large area surface morphology and thickness change of assembled multilayer film (9.5 bilayers) were also examined by SEM. The quartz substrate was cleaved and separated into two parts after a "freeze-fractured" process. One part of the substrate remained untreated as a control while the other part was immersed into a bath of acidic solution (pH 2.75 diluted HCl) for 30 min followed by a 20 s rinse with ultrapure water. The films were then heated at 120 °C for 2 h to lock the structure prior to the SEM observation. However, the thickness of 9.5 bilayers film (pH = 6) measured from SEM cross-section image is 150.3 nm (Figure 9A). It appears that the film thicknesses obtained from the two measurements (SEM and QCM) are in quite disagreement. Since SEM cross-section thickness is visible and more credible, the experiential equation mentioned above may not suitable for the star polymer system. The film thickness measured from the scratched step height by AFM was about 135 nm, which is in good agreement with the thickness measured by SEM (see Figure 6 of Supporting Information). The average thickness of untreated film is estimated at about 150 nm, and the surface exhibits a rather dense texture (Figure 9A,C). For the post-pH-treated film, the film changes dramatically to a nanoscale or even microporous structure, with pores in diameter ranging from approximately 300 nm to 1.8 μm (Figure 9D). The microporous surface morphology is quite similar to that of post-pH-treated (pH 3.0) layer-by-layer multilayers consisting of linear poly(ethylenimine) (LPEI) and poly(acrylic acid) (PAA), which has been described as isolated craters.[38] The thickness of the post-treated porous film is more than double of the original film, reaching up to 328 nm (Figure 9B). Meanwhile, it is interesting to find that the film in SEM images turns to be brighter after the porosity transformation at pH 2.75, which may due to the changing of pore conductive surface on the cross section of the film, hence changing of the electrons in SEM measurement. Given the conservation of mass in the films during the porosity transformation undergoing the pH 2.75 immersion, the pore volume of 21-arm star PDMAEMA/PSS film system (assembled at pH 6/6) is estimated at 53% according to the previous reports.[39,40]

Conclusions

The synthesis of controlled star PDMAEMA with different molecular weight and arm number (21, 14, and 7) was achieved by ATRP through the "core-first" method. The pH-responsive behavior of star PDMAEMA was demonstrated by DLS in solution. It is anticipated that the LbL assembled thin films could

preserve the pH-responsivity when the star polymers are constructed into the films, which will be of great benefit for potential biomedical applications, especially for LbL films containing biological components. Herein, the effects of molecular weight and arm number of star polymers on the formation and morphology changes in response to the post-pH treatment of LbL films were investigated. It is found that star polymers with certain arm number deposit more mass with the increase of molecular weight. The film assembled from 14-arm star PDMAEMA exhibits the fastest growth and the most dramatic pH-dependent morphology change with pore diameter up to 2 μm upon the post-acidic treatment. The different charge density and the degree of intermingling between star polymers within the film are considered to be the main factor which determines the formation and the pH-dependent properties of multilayer films. Current work is underway to investigate self-regulated drug delivery systems based on LbL films fabricated with star polymers, insulin, and glucose oxidase.

Acknowledgment. We thank Prof. Hua Ai for technical support and helpful suggestions. The financial support from the National Natural Science Foundation of China (20704026) and Fok Ying Tong Education Foundation (122034) is greatly appreciated.

Supporting Information Available: Additional details of the synthesis of star polymers and the film thickness measurement. This material is available free of charge via the Internet at http://pubs.acs.org.

References and Notes

(1) Decher, G. *Science* **1997**, *277*, 1232–1237.
(2) Hammond, P. T. *Adv. Mater.* **2004**, *16*, 1271–1293.
(3) Boudou, T.; Crouzier, T.; Ren, K.; Blin, G.; Picart, C. *Adv. Mater.* **2010**, *22*, 441–467.
(4) Kaschak, D. M.; Mallouk, T. E. *J. Am. Chem. Soc.* **1996**, *118*, 4222–4223.
(5) Khopade, A. J.; Caruso, F. *Nano Lett.* **2002**, *2*, 415–418.
(6) Mamedov, A. A.; Kotov, N. A.; Prato, M.; Guldi, D. M.; Wicksted, J. P.; Hirsch, A. *Nature Mater.* **2002**, *1*, 190–194.
(7) Lvov, Y.; Decher, G.; Sukhorukov, G. *Macromolecules* **1993**, *26*, 5396–5399.
(8) Caruso, F.; Möhwald, H. J. *J. Am. Chem. Soc.* **1999**, *121*, 6039–6046.
(9) Yoo, P. J.; Nam, K. T.; Qi, J.; Lee, S. K.; Park, J.; Belcher, A. M.; Hammond, P. T. *Nature Mater.* **2006**, *5*, 234–240.
(10) Khopade, A. J.; Caruso, F. *Biomacromolecules* **2002**, *3*, 1154–1162.
(11) Lowman, G. M.; Hammond, P. T. *Small* **2005**, *1*, 1070–1073.
(12) Zhang, J.; Senger, B.; Vautier, D.; Picart, C.; Schaaf, P.; Voegel, J. C.; Lavalle, P. *Biomaterials* **2005**, *26*, 3353–3361.
(13) Liu, J.; Cheng, L.; Song, Y.; Liu, B.; Dong, S. *Langmuir* **2001**, *17*, 6747–6750.
(14) Calvo, E. J.; Danilowicz, C.; Lagier, C. M.; Manrique, J.; Otero, M. *Biosens. Bioelectron.* **2004**, *19*, 1219–1228.
(15) Messina, R. *Macromolecules* **2004**, *37*, 621–629.
(16) Schlnoff, J. B.; Dubas, S. T. *Macromolecules* **2001**, *34*, 592–598.
(17) Blasini, D. R.; Flores-Torres, S.; Smilgies, D. M.; Abruña, H. D. *Langmuir* **2006**, *22*, 2082–2089.
(18) Yang, S.; Zhang, Y.; Wang, C.; Hong, S.; Xu, J.; Chen, Y. *Langmuir* **2006**, *22*, 338–343.
(19) Connal, L. A.; Li, Q.; Quinn, J. F.; Tjipto, E.; Caruso, F.; Qiao, G. G. *Macromolecules* **2008**, *41*, 2620–2626.
(20) Kim, B.-S.; Gao, H.; Argun, A. A.; Matyjaszewski, K.; Hammond, P. T. *Macromolecules* **2009**, *42*, 368–375.
(21) Braunecker, W. A.; Matyjaszewski, K. *Prog. Polym. Sci.* **2007**, *32*, 93–146.
(22) Gao, H.; Matyjaszewski, K. *Macromolecules* **2006**, *39*, 3154–3160.
(23) Li, J.; Xiao, H.; Kim, Y. S.; Lowe, T. L. *J. Polym. Sci., Part A: Polym. Chem.* **2005**, *43*, 6345–6354.
(24) Li, J.; Guo, Z.; Xin, J.; Zhao, G.; Xiao, H. *Carbohydr. Polym.* **2010**, *79*, 277–283.
(25) Guo, Z.; Chen, X.; Zhang, X.; Xin, J.; Li, J.; Xiao, H. *Tetrahedron Lett.* **2010**, *51*, 2351–2353.
(26) Zhang, X.; Xia, J.; Matyjaszewski, K. *Macromolecules* **1998**, *31*, 5167–5169.
(27) Mao, B.; Gan, L.-H.; Gan, Y.-Y.; Li, X.; Ravi, P.; Tam, K.-C. *J. Polym. Sci., Part A: Polym. Chem.* **2004**, *42*, 5161–5169.
(28) Mao, B.; Gan, L.-H.; Gan, Y.-Y. *Polymer* **2006**, *47*, 3017–3020.
(29) van de Watering, P.; Moret, E. E.; Schuurmans-Nieuwenbroek, N. M. E.; van Steenbergen, M. J.; Hennink, W. E. *Bioconjugate Chem.* **1999**, *10*, 589–597.
(30) Picart, C.; Mutterer, J.; Richert, L.; Luo, Y.; Prestwich, G. D.; Schaaf, P.; Voegel, J.-C.; Lavalle, P. *Proc. Natl. Acad. Sci. U.S.A.* **2002**, *99*, 12531–12535.
(31) Kujawa, P.; Moraille, P.; Sanchez, J.; Badia, A.; Winnik, F. M. *J. Am. Chem. Soc.* **2005**, *127*, 9224–9234.
(32) Tedeschi, C.; Caruso, F.; Möhwald, H.; Kirstein, S. *J. Am. Chem. Soc.* **2000**, *122*, 5841–5848.
(33) Lvov, Y.; Ariga, K.; Ichinose, I.; Kunitake, K. *J. Am. Chem. Soc.* **1995**, *117*, 6117–6123.
(34) Shiratori, S. S.; Rubner, M. F. *Macromolecules* **2000**, *33*, 4213–4219.
(35) Porcel, C.; Lavalle, Ph.; Decher, G.; Senger, B.; Voegel, J.-C.; Schaaf, P. *Langmuir* **2007**, *23*, 1898–1904.
(36) Sun, B.; Jewell, C. M.; Fredin, N. J.; Lynn, D. M. *Langmuir* **2007**, *23*, 8452–8459.
(37) Tokarev, I.; Minko, S. *Adv. Mater.* **2009**, *21*, 241–247.
(38) Lutkenhaus, J. L.; McEnnis, K.; Hammond, P. T. *Macromolecules* **2008**, *41*, 6047–6054.
(39) Yoo, D.; Shiratori, S. S.; Rubner, M. F. *Macromolecules* **1998**, *31*, 4309–4318.
(40) Mendelsohn, J. D.; Barrett, C. J.; Chan, V. V.; Pal, A. J.; Mayes, A. M.; Rubner, M. F. *Langmuir* **2000**, *16*, 5017–5023.